

Space-Time Covariance Functions based on Linear Response Theory and the Turning Bands Method*

Dionissios T. Hristopulos, ^{†1} and Ivi C. Tsantili^{‡2}

¹Geostatistics Laboratory, School of Mineral Resources Engineering,
Technical University of Crete, Chania, 73100 Greece

²Beijing Computational Science Research Center, Beijing, 100193 China

October 10, 2018

Abstract

The generation of non-separable, physically motivated covariance functions is a theme of ongoing research interest, given that only a few classes of such functions are available. We construct a non-separable space-time covariance function based on a diffusive Langevin equation. We employ ideas from statistical mechanics to express the response of an equilibrium (i.e., time independent) random field to a driving noise process by means of a linear, diffusive relaxation mechanism. The equilibrium field is assumed to follow an exponential joint probability density which is determined by a spatial local interaction model. We then use linear response theory to express the temporal evolution of the random field around the equilibrium state in terms of a Langevin equation. The latter yields an equation of motion for the space-time covariance function, which can be solved explicitly at certain limits. We use the explicit covariance model obtained in one spatial dimension and time. By means of the turning bands transform, we derive a non-separable space-time covariance function in three space dimensions and time. We investigate the mathematical properties of this space-time covariance function, and we use it to model a dataset of daily ozone concentration values from the conterminous USA.

Keywords: Langevin equations; Spartan random fields; turning bands; marginal variogram; biharmonic; ozone mapping

*This manuscript is a preprint of an article submitted for publication in Journal of Spatial Statistics, <http://www.journals.elsevier.com/spatial-statistics>

[†]dionisi@mred.tuc.gr.; Corresponding author

[‡]ivi.tsantili@gmail.com

1 Introduction

The formulation of mathematically valid and physically motivated covariance functions is an ongoing pursuit in spatiotemporal statistics [6, 7, 15, 8]. This is driven by the central role of covariance functions in the estimation and simulation of space-time processes. In particular, there is strong interest in formulating non-separable space-time covariance models. This research is motivated first by the inadequacy of separable covariance models to capture the patterns in realistic space-time data [7, 35]. Secondly, space-time random fields often represent the evolution of physical variables under a respective partial differential equation (PDE) with stochastic components (e.g. initial or boundary conditions, coefficients, or driving noise) [37, 16, 40, 24]. Even in simple cases, this evolution leads to the development of non-separable space-time covariance functions. A case in point is the one-dimensional diffusion of an initially parabolic concentration field in a medium with uniform but random diffusion coefficient [7]. This problem illustrates how the non-separability of the covariance function emerges from the superposition of separable space-time eigenfunctions.

Since the explicit solution of PDEs is in many cases not feasible, non-separable covariances have also been constructed by employing mathematical permissibility criteria, thus circumventing the problem of solving an underlying PDE, e.g. [15, 9, 30, 26]. Another possibility for constructing space-time covariance functions is by integrating permissible spectral densities. However, the explicit integration of the spectral density is not feasible in many cases [35]. Recent reviews of spatiotemporal covariance functions are given in [26, 31, 8].

As argued above, space-time covariance functions can be obtained as solutions to PDEs. These PDEs are associated with respective stochastic partial differential equations (SPDEs), also known as Langevin equations, that describe the evolution of the corresponding space-time random field [21]. This perspective was used by Whittle to derive the spatial Whittle-Matérn covariance functions [37]. Another example is the space-time covariance function developed by Heine as a solution of a parabolic SPDE with one time and one space dimension [16]. The connection between rational spectral densities and Langevin equations that represent the corresponding random field is also discussed by Yaglom [39]. The same perspective was also pursued by engineers to develop methods for the control of systems with random parameters [14].

Various approaches for the construction of covariance functions are possible in a framework that involves partial differential equations. These equations may pertain to the evolution of the random field, in which case they constitute stochastic partial differential equations, or they may describe the dynamics of the covariance function, in which case they are deterministic partial differential equations.

The *SPDE approach* aims to efficiently generate random fields which obey the Whittle-Matérn covariance. In the SPDE method, the random field that satisfies the Langevin equation associated with the Whittle-Matérn covariance family is solved using a projection to a finite-dimensional function base [29]. The SPDE method can also be used to generate non-stationary random fields [28]. To our knowledge this approach has not been extended to explicitly include random fields with space-time covariance functions.

The *covariance PDE* approach focuses on deriving space-time covariance functions by solving suitable PDEs. If the SPDE equation that determines the evolution of the studied process driven by noise is known, it can be used to derive an associated covariance PDE which represents the equation of motion (EOM) of the covariance function. If the initial SPDE is linear, so is the associated PDE for the covariance function. For stationary systems the covariance PDE is defined over the domain $\mathcal{D} \in \mathbb{R}^d \times \mathbb{R}$ of spatial and temporal lags. Hence, the derivatives are taken with respect to the spatial and temporal lags instead of the position and time. This approach has been used in statistical physics to study dynamic critical phenomena in ideal systems where the structure of the SPDE is assumed to be known [17].

Often, the Langevin equations (SPDEs) that determine the dynamic evolution of the studied process are not known. In such cases, the equation of motion of the covariance can not be derived from first principles. In other cases, the respective covariance PDEs may be known but unsolvable by analytical means. Then, one feasible solution is to use a flexible enough *surrogate PDE* to model space-time correlations. This approach was followed in the development of Spartan spatial random fields [18, 20] and their space-time extensions [21].

The physical justification of surrogate PDEs is that they can provide tractable, albeit idealized, models for space-time correlations which approximate the behavior of broad classes of stochastic systems. For example, Heine [16] considered SPDEs of elliptic, parabolic, and hyperbolic types which conform with the standard classification of partial differential equations with second-order partial derivatives [10]. The types above are respectively associated with equilibrium (steady-state), diffusive, and wave propagation processes. Hence, solutions for covariance functions that correspond to SPDEs of these types can provide useful approximations for general processes with the above characteristics. In a sense, the idea of using surrogate models is not new in spatial statistics: all the classical covariance functions represent plausible but simplified forms of spatial dependence which can be used to model, even if approximately, various patterns of spatial (or spatiotemporal) dependence.

In simple cases the covariance PDEs (either exact or surrogate) are linear and can be solved explicitly, at least for certain choices of initial and boundary conditions. Explicit solution of covariance PDEs was successfully employed in the

Whittle-Matérn case [37], in the Heine covariance model [16], and in the case of Spartan spatial random fields [20, 19]. Explicit results for space-time covariance functions were also recently derived using the tools of linear response theory [21]. The linear response theory and the Heine approach involve different theoretical frameworks. However, in one spatial dimension the linear response theory of the Spartan spatial random field recovers at the zero-curvature limit the parabolic Heine covariance model.

If the covariance PDE (exact or surrogate) is not amenable to explicit solution, approximate space-time covariance functions can be obtained by applying model order reduction techniques. Covariance PDEs based on model order reduction simplify the mathematical problems using Galerkin projections of the solution on finite-dimensional bases [10]. Order reduction methods have been used in engineering mechanics to develop expansions of random fields when the dynamic equations satisfied by the field are known [14, 38]. Order reduction methods are broadly based on the same idea as the SPDE approach. Once the reduced-order random field representation is known, approximations of the covariance function can also be derived using the most important basis functions.

Herein we construct a space-time covariance function based on the surrogate PDE approach. The PDE is obtained within the statistical mechanics framework of linear response theory. Our starting point is an equilibrium Spartan spatial random field (SSRF) [23]. This leads to a parabolic PDE for the covariance function, which is suitable for diffusive processes. The remainder of this document is structured as follows: Section 2 presents an overview of the linear response theory leading to an equation of motion for the space-time covariance function. Section 3 presents the solution of the above equation in $1 + 1$ dimensions, its transformation using the turning bands method to a $3 + 1$ non-separable covariance function, and an investigation of its properties. This section includes the new space-time covariance function (9) which is the main closed-form result obtained in this work. Section 4 develops the corresponding variogram function and obtains the respective space and time marginal variogram functions. Section 5 focuses on the estimation of the new covariance parameters from space-time data using the method of marginal space and time variograms. These are used to model the distribution of daily ozone values in the USA over a period of fourteen days in Section 6. Finally, we present our conclusions and a discussion of the results in Section 7.

2 Review of Linear Response Theory

This section briefly reviews the main steps of the application of linear response theory in the construction of space-covariance functions following [21].

Let us denote by $X(\mathbf{s}, t)$ the space-time random field at the space time point $(\mathbf{s}, t) \in \mathbb{R}^d \times \mathbb{R}$, and by $X(\mathbf{s})$ the static field at equilibrium (in the absence of temporal fluctuations). Realizations of the field will be denoted by the lowercase letter $x(\mathbf{s})$. The expectation over the ensemble of states of the field will be denoted by means of $\mathcal{E}[\cdot]$. The spatial domain of interest is $\mathcal{D}_s \subset \mathbb{R}^d$ and the temporal domain of interest $\mathcal{D}_T \subset \mathbb{R}$.

2.1 The equilibrium state

The equilibrium (static) regime provides an initial condition on the space-time covariance function. Since we are interested in covariance functions, we will focus on zero-mean random fields. First, we assume that the field realizations in equilibrium are determined by the Gibbs probability density function (pdf) with the following exponential form

$$f_X(\mathbf{x}; \boldsymbol{\theta}) = Z^{-1}(\boldsymbol{\theta}) e^{-\mathcal{H}(\mathbf{x}; \boldsymbol{\theta})},$$

where $\mathcal{H}(\mathbf{x}; \boldsymbol{\theta})$ is a quadratic, non-negative functional of the field states (realizations) $\mathbf{x} = (x_1, \dots, x_N)^\top$ at N points $\mathbf{s}_i \in \mathbb{R}^d$, where $i = 1, \dots, N$, the superscript T denotes the transpose, $\boldsymbol{\theta}$ is the parameter vector, and $Z(\boldsymbol{\theta})$ is the partition function which normalizes the joint density.

In the continuum limit \mathbf{x} is replaced by the field $x(\mathbf{s})$ which is defined at every site \mathbf{s} on the spatial domain \mathcal{D}_s . The spatial correlations of the field realization $x(\mathbf{s})$ are implemented by means of the surrogate functional $\mathcal{H}[x(\mathbf{s}); \boldsymbol{\theta}]$ which depends on the values of the realization $x(\mathbf{s})$ for all $\mathbf{s} \in \mathcal{D}$. For the energy functional we use the SSRF form [18] with an additional parameter μ as follows

$$\mathcal{H}[x(\mathbf{s}); \boldsymbol{\theta}] = \frac{1}{2\eta_0 \xi^d} \int_{\mathbb{R}^d} ds \left\{ [x(\mathbf{s})]^2 + \eta_1 \xi^2 [\nabla x(\mathbf{s})]^2 + \mu \xi^4 [\nabla^2 x(\mathbf{s})]^2 \right\}, \quad (1)$$

where $\boldsymbol{\theta} = (\eta_0, \eta_1, \xi, \mu)^\top$. In the energy function (1) the first term in the integrand measures the square of the fluctuations, the second term is proportional to the square gradient, and the third term to the square of the curvature (we assume that the curvature is represented by the Laplacian). The coefficients in (1) are selected so that the ‘‘energy’’ $\mathcal{H}[x(\mathbf{s}); \boldsymbol{\theta}]$ is dimensionless. Hence, the *characteristic length* ξ has units of length, the *rigidity* η_1 is a dimensionless number which determines the resistance of $x(\mathbf{s})$ to bending, while η_0 has the units $[X]^2$. Finally, the new dimensionless parameter $\mu \geq 0$ controls the contribution of the curvature term. We refrain from calling ξ the correlation length, because the presence of η_1 implies that the relation of ξ with the correlation length is more complex than for simpler models [22].

The permissibility conditions imposed by Bochner's theorem [3] constraints for the values of η_1 . For $\mu = 1$ the permissibility condition is $\eta_1 > -2$. For $\mu = 0$, however, the respective condition is more stringent since it requires $\eta_1 > 0$. We will henceforth assume $\eta_1 > 0$ to account for all possible values of η_1 .

2.2 The linear response Langevin equation

The premise of linear response theory is that the dynamic evolution of the system near the equilibrium state is essentially determined by $\mathcal{H}[x(\mathbf{s}); \boldsymbol{\theta}]$. In particular, if noise tends to drive the system away from the equilibrium, the system will develop in response a restoring velocity that depends on the departure from the equilibrium. The response is described in terms of the following Langevin equation

$$\frac{\partial x(\mathbf{s}, t)}{\partial t} = -\Gamma \left. \frac{\delta \mathcal{H}[x(\mathbf{s}); \boldsymbol{\theta}]}{\delta x(\mathbf{s})} \right|_{x(\mathbf{s})=x(\mathbf{s}, t)} + \zeta(\mathbf{s}, t), \quad (2)$$

where $\Gamma > 0$ is a diffusion coefficient that determines the relaxation towards the equilibrium, $\delta(\cdot)/\delta x(\mathbf{s})$ is the functional derivative with respect to the field realization, and $\zeta(\mathbf{s}, t)$ is the noise field. For the latter, we assume that it is a Gaussian white noise with $\mathcal{E}[\zeta(\mathbf{s}, t)] = 0$ and $\mathcal{E}[\zeta(\mathbf{s}, t)\zeta(\mathbf{s}', t')] = D$, where $D > 0$ is the variance, and $\mathcal{E}[\cdot]$ denotes the expectation with respect to the noise.

Equation (2) essentially determines the rate at which the random field realizations change in time as a superposition of two terms: the first component is the relaxation component which tends to restore the equilibrium, while the second component is a stochastic velocity that perturbs the approach to equilibrium.

2.3 Equation of motion of the linear response covariance function

A number of technical steps described in [21] lead to the following partial differential equation that determines the motion of the covariance function

$$\frac{\partial C(\mathbf{s} - \mathbf{s}', t - t'; \boldsymbol{\theta})}{\partial \tau} = -\Gamma \text{sign}(\tau) \mathcal{E} \left[x(\mathbf{s}, t) \left. \frac{\delta \mathcal{H}[x(\mathbf{s}); \boldsymbol{\theta}]}{\delta x(\mathbf{s}')} \right|_{x(\mathbf{s}')=x(\mathbf{s}', t')} \right]. \quad (3)$$

In the above, $\tau = t - t' \in T$ is the temporal lag. The sign function is defined by $\text{sign}(\tau) = 1$ if $\tau > 0$, $\text{sign}(\tau) = -1$ if $\tau < 0$, and $\text{sign}(\tau) = 0$ if $\tau = 0$. The subscript $x(\mathbf{z}) = x(\mathbf{s}', t')$ denotes that after the functional derivative is calculated, the static realization $x(\mathbf{s}')$ is replaced by the dynamic realization $x(\mathbf{s}', t')$. The vector $\boldsymbol{\theta}$ includes a general set of parameters; the parameter Γ can be absorbed in the amplitude coefficient of $\mathcal{H}[x(\mathbf{s}); \boldsymbol{\theta}]$, i.e., in η_0 .

Next, we replace $\mathcal{H}[x(\mathbf{s}); \boldsymbol{\theta}]$ in equation (3) with the Spartan energy functional (1), evaluate the functional derivatives, and calculate the resulting field expectations (see [21]). Then, the covariance equation of motion is given by the following linear PDE which includes fourth-order spatial derivatives

$$\frac{\partial C_{\mathbf{x}}(\mathbf{r}, \tau; \boldsymbol{\theta}')}{\partial \tau} = -\frac{\text{sign}(\tau)}{\tau_c} (1 - \eta_1 \xi^2 \nabla^2 + \mu \xi^4 \nabla^4) C_{\mathbf{x}}(\mathbf{r}, \tau; \boldsymbol{\theta}'), \quad (4)$$

with suitable boundary and initial conditions which are defined below. We will refer to it as the Spartan linear response PDE.

The function $C_{\mathbf{x}}(\mathbf{r}, \tau; \boldsymbol{\theta}') : \mathbb{R}^d \times T \rightarrow \mathbb{R}$ is the space-time covariance function associated with the linear response of the Spartan energy functional, $\mathbf{r} = \mathbf{s} - \mathbf{s}' \in \mathbb{R}^d$ denotes the spatial lag, and $\boldsymbol{\theta}' = (\eta_0, \eta_1, \xi, \mu, \tau_c)$ is the parameter vector of the covariance function. The *characteristic time constant* τ_c is linked to the noise variance and the SSRF parameters by means of $\tau_c = D/2\eta_0\xi^d$. In addition, $\nabla^2 = \sum_{i=1}^d \partial^2 / \partial r_i^2$ denotes the Laplacian operator, and its square $\nabla^4 = (\nabla^2)^2$ is the biharmonic operator [10]. The dependence on η_0 is introduced via the initial condition as shown below.

In the Spartan linear response PDE (4) the term proportional to ∇^2 is derived via the functional differentiation from the $\mathcal{H}[x(\mathbf{s})]$ component that involves the integral of the square gradient $[\nabla x(\mathbf{s})]^2$, whereas the term proportional to ∇^4 is obtained from the term proportional to the integral of the square curvature $[\nabla^2 x(\mathbf{s})]^2$ of the field over \mathcal{D}_s .

2.4 Solution of the Spartan linear response PDE based on the spectral method

Assuming that \mathcal{D}_s expands to an infinite support, the *boundary conditions* are that $C_{\mathbf{x}}(\mathbf{r}, \tau; \boldsymbol{\theta}')$ tends to zero as $\|\mathbf{r}\| \rightarrow \infty$ (unbounded domain). Then, the Spartan linear response PDE (4) is best solved by applying the Fourier integral transform method [25] to the spatial component of the covariance function. The *spatial Fourier transform* of the covariance function is given by

$$\tilde{C}(\mathbf{k}, \tau; \boldsymbol{\theta}') = \mathcal{F}_{\mathbf{r}}[C(\mathbf{r}, \tau; \boldsymbol{\theta}')] = \int_{\mathbb{R}^d} d\mathbf{r} e^{-j\mathbf{k}\cdot\mathbf{r}} C(\mathbf{r}, \tau; \boldsymbol{\theta}'),$$

where the function $\tilde{C}(\mathbf{k}, \tau; \boldsymbol{\theta}')$ is the time-dependent spectral density where $\mathbf{k} \in \mathbb{R}^d$ is the wavevector in reciprocal space. The *inverse Fourier transform (IFT)* is then given by

$$C(\mathbf{r}, \tau; \boldsymbol{\theta}') = \mathcal{F}_{\mathbf{k}}^{-1}[\tilde{C}(\mathbf{k}, \tau; \boldsymbol{\theta}')] = \frac{1}{(2\pi)^d} \int_{\mathbb{R}^d} d\mathbf{k} e^{j\mathbf{k}\cdot\mathbf{r}} \tilde{C}(\mathbf{k}, \tau; \boldsymbol{\theta}').$$

Inserting the IFT in the Spartan linear response PDE (4) leads to the following *first-order ordinary differential equation (ODE)* with respect to time with initial condition $\tilde{C}(\mathbf{k}, 0)$

$$\frac{\partial \tilde{C}(\mathbf{k}, \tau; \boldsymbol{\theta}')}{\partial \tau} = -\frac{\text{sign}(\tau)}{\tau_c} (1 + \eta_1 k^2 \xi^2 + \mu k^4 \xi^4) \tilde{C}(\mathbf{k}, \tau; \boldsymbol{\theta}'). \quad (5a)$$

The above ODE is solved using the statistically homogeneous and isotropic *initial condition*. This is provided by the Spartan spectral density which corresponds to the equilibrium random field [18], i.e.,

$$\tilde{C}(\|\mathbf{k}\|, 0; \boldsymbol{\theta}') := \tilde{G}(\mathbf{k}) = \frac{\eta_0 \xi^d}{1 + \eta_1 (\|\mathbf{k}\| \xi)^2 + \mu (\|\mathbf{k}\| \xi)^4}, \quad (5b)$$

where $\|\mathbf{k}\| \in \mathbb{R}_+$ is the wavenumber, i.e., the Euclidean norm of the reciprocal-space wavevector \mathbf{k} .

The solution of the linear ODE (5a) for the time-dependent spectral density is given by the exponential function

$$\tilde{C}(\|\mathbf{k}\|, \tau; \boldsymbol{\theta}') = \tilde{G}(\mathbf{k}) e^{-(1 + \eta_1 \|\mathbf{k}\|^2 \xi^2 + \mu \|\mathbf{k}\|^4 \xi^4) |\tau| / \tau_c}. \quad (6)$$

Real-space solutions are obtained by evaluating the inverse Fourier transform of (6) using the isotropic spectral representation [40].

2.4.1 The zero-curvature limit

For $\mu = 0$ (zero-curvature model), the covariance equation of motion (4) is a *second-order PDE of the parabolic type*. In [21] we solved this PDE using the Fourier integral transform method [25]. The expressions derived for the covariance function in real space depend on the dimensionality d . For $d = 2, 3$ the derived functions have singularities at the origin. In contrast, the covariance function is well defined in $d = 1$.

2.5 Properties of solutions of the Spartan linear response PDE

Properties of the functions $C_x(\mathbf{r}, \tau; \boldsymbol{\theta}')$ that solve the Spartan linear response PDE (4) can be investigated, even if explicit forms of the solutions are not available.

1. Space-time covariance functions generated by the linear response of the Spartan energy functional are statistically homogeneous in space and stationary in time. These properties are due to the choices of infinite support, constant coefficients, and homogeneous initial condition.

2. In addition, the solution is $C_x(\mathbf{r}, \tau; \boldsymbol{\theta}')$ isotropic, because neither the Spartan linear response PDE (4) nor the initial condition (5b) distinguish between different spatial directions. This constraint can in principle be easily relaxed by replacing $\|\mathbf{k}\| \xi$ in the ODE and the initial condition (5) with $\sum_{i=1}^d k_i \xi_i$. In the anisotropic case, however, the analytical evaluation of the inverse Fourier transform has not been done.
3. A bounded domain with non-periodic boundary conditions will lead to non-homogeneous covariance functions. Explicit solutions would be more difficult to obtain in such cases.

3 Space-Time Covariance Functions by means of the Turning Bands Method

In this section, we apply the turning bands method to the one dimensional (in space) covariance function (7). This operation generates a permissible space-time covariance function in three spatial dimensions and time.

3.1 Space-time covariance function in 1 + 1 dimensions

The one-dimensional space-time covariance function $C_1(r, \tau)$ based on the surrogate Spartan functional $\mathcal{H}[x(\mathbf{s}); \boldsymbol{\theta}]$ defined by (1) is given by the following expression

$$C_1(h, u; \tilde{\boldsymbol{\theta}}) = \frac{\eta_0 \lambda}{4} \left[e^{-\lambda h} \operatorname{erfc} \left(\sqrt{u} - \frac{\lambda h}{2\sqrt{u}} \right) + e^{\lambda h} \operatorname{erfc} \left(\sqrt{u} + \frac{\lambda h}{2\sqrt{u}} \right) \right]. \quad (7)$$

In the above, $h = |r|/\xi$ and $u = |\tau|/\tau_c$ are the normalized space and time lags and $\tilde{\boldsymbol{\theta}} = (\eta_0, \lambda, \xi, \tau_c)^\top$ is the parameter vector. The *flexibility (inverse rigidity)* constant is $\lambda = 1/\sqrt{\eta_1}$, and $\operatorname{erfc}(\cdot)$ is the complementary error function defined by the following integral

$$\operatorname{erfc}(x) = \frac{2}{\sqrt{\pi}} \int_x^\infty dt e^{-t^2}.$$

The equation (7) recaptures the covariance model of Heine [16, 24], albeit with a different parametrization.

3.2 Turning bands method

Space transforms are mathematical operations that can generate higher-dimensional functions based on lower-dimensional projections [11]. In particular, Matheron developed the *turning bands method* which can be used to produce higher-dimensional isotropic covariance and generalized covariance functions from one-dimensional covariances [33].

We briefly describe the turning bands method following the presentation in [33]. Let $Y(t)$, where $t \in \mathbb{R}$ be a one-dimensional random process with covariance function $C_1(t - t')$ and let $\mathbf{p} \in \mathbb{R}^d$ be a unit random vector with $\|\mathbf{p}\| = 1$. Moreover, let an isotropic random field $X(\mathbf{s})$, where $\mathbf{s} \in \mathbb{R}^d$ be such that $Y(t) = X_{\mathbf{p}}(\mathbf{s}) = X(\mathbf{s} \cdot \mathbf{p})$ is the one-dimensional projection of $X(\mathbf{s})$ along the vector \mathbf{p} . The covariance function of the projection of the random field $X(\mathbf{s})$ is given by

$$\mathcal{E} [X_{\mathbf{p}}(\mathbf{s}) X_{\mathbf{p}}(\mathbf{s}')] = C_1(\mathbf{p} \cdot (\mathbf{s} - \mathbf{s}')).$$

The covariance of $X(\mathbf{s})$ can be evaluated by calculating the average over one-dimensional projections along all different directions \mathbf{p} , i.e.,

$$C(\|\mathbf{r}\|) = \int_{B_d} d\mathbf{p} C_1(\mathbf{p} \cdot \mathbf{r}) \pi(\mathbf{p}),$$

where $\pi(\mathbf{p})$ is the probability density function representing the distribution of the unit vector \mathbf{p} , and B_d denotes that the space integral is evaluated over the surface of the unit sphere. Then it follows that

$$C_d(\|\mathbf{r}\|) = \frac{2\Gamma(d/2)\pi^{-1/2}}{\Gamma(\frac{1}{2}(d-1))} \int_0^1 C_1(v\|\mathbf{r}\|) (1-v^2)^{(d-3)/2}. \quad (8)$$

3.3 Non-separable space-time covariance function

In light of the above, and in particular equation (8), a *three-dimensional, isotropic covariance* function is generated from $C_1(r, \tau)$ by means of the following integral (see also [32])

$$C_3(\|\mathbf{r}\|, \tau; \tilde{\boldsymbol{\theta}}) = \frac{1}{\|\mathbf{r}\|} \int_0^{\|\mathbf{r}\|} dx C_1(x, \tau; \tilde{\boldsymbol{\theta}}) = \frac{1}{h} \int_0^h dy C_1(y, u; \tilde{\boldsymbol{\theta}}),$$

where $C_1(\cdot, \cdot; \tilde{\boldsymbol{\theta}})$ is given by (7). The above integral requires the integration the $\text{erfc}(x)$ function, which we perform using integral tables [34]. The integration leads to the following *non-separable* space-time covariance function

$$C_3(h, u; \tilde{\boldsymbol{\theta}}) = \frac{\eta_0}{4h} \left[2e^{-u} \operatorname{erf} \left(\frac{\lambda h}{2\sqrt{u}} \right) + e^{\lambda h} \operatorname{erfc} \left(\sqrt{u} + \frac{\lambda h}{2\sqrt{u}} \right) - e^{-\lambda h} \operatorname{erfc} \left(\sqrt{u} - \frac{\lambda h}{2\sqrt{u}} \right) \right], \quad (9)$$

where $h = \|\mathbf{r}\|/\xi$ is the normalized spatial lag, $u = |\tau|/\tau_c$, is the normalized time lag, $\operatorname{erfc}(x)$ is the complementary error function, and $\operatorname{erf}(x) = 1 - \operatorname{erfc}(x)$, is the error function. The above is the space-transformed image of the 1 + 1 zero-curvature, linear response covariance function (7). Hence, we will refer to it as the “*Space-Transformed Spartan Linear Response*” or STSLR covariance function.

3.4 Properties of the STSLR space-time covariance function

In this section we investigate some properties of the space-transformed image of the 1 + 1 zero-curvature, linear response covariance function. As we have already noted above, the STSLR covariance function (9) is *non-separable, stationary in time, and spatially isotropic*. In the following, we drop the dependence of the covariance function on $\tilde{\boldsymbol{\theta}}$ for notational brevity.

A general class of non-separable space-time covariance functions is provided by the isotropic Gneiting family [15],

$$C(h, u) = \frac{\alpha^2}{\psi(u^2)^\delta} \phi \left(\frac{h^2}{\psi(u^2)} \right),$$

where $\phi(\cdot)$ is a completely monotone function, $\psi(\cdot)$ is a Bernstein function (i.e., a positive function with completely monotone derivative), $\alpha > 0$ and $\delta > d/2$. Both $\phi(\cdot)$ and $\psi(\cdot)$ satisfy appropriate boundary conditions at zero and infinity. We note that the STSLR covariance has a space-time dependence which is not included in the broad class of Gneiting functions.

The STSLR model also differs from the extension of the Heine $\mathbb{R} \times T$ model to $\mathbb{R}^d \times T$ which was proposed by Ma [30, 35]; in addition to the different arguments of the complementary error function, the STSLR model includes a third term which involves the error function.

3.4.1 Symmetry

The STSLR covariance function (9) depends on the spatial and temporal lags only through their magnitudes. Hence, it satisfies the properties $C_3(\mathbf{r}, \tau) = C_3(-\mathbf{r}, \tau)$ and $C_3(\mathbf{r}, \tau) = C_3(\mathbf{r}, -\tau)$ and is a *fully symmetric covariance function* according to [15, 27]. The contours of $C_3(\mathbf{r}, \tau)$ in the domain $\mathbb{R} \times T$ are shown in Fig. 1.

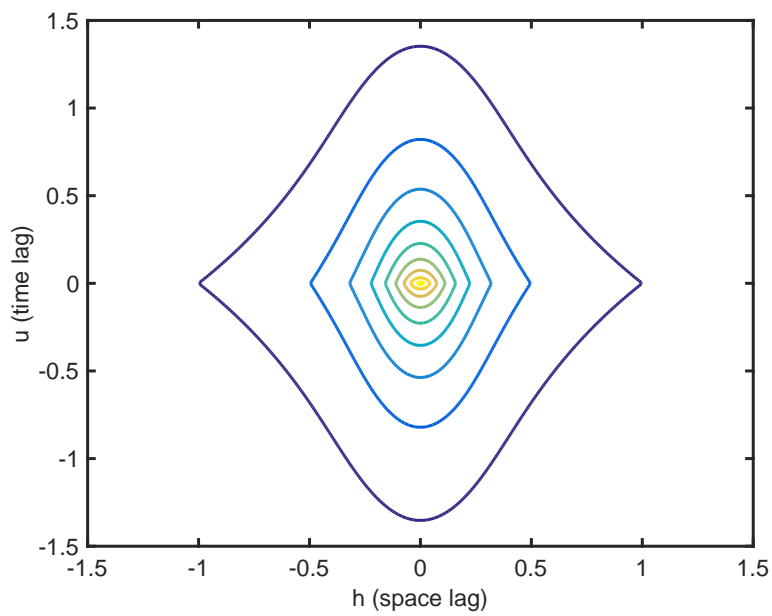


Figure 1: Contour plots of the STSLR space-time covariance function (9) generated by applying the turning bands method to the $1 + 1$ covariance function (7) which is obtained by the linear response of the zero-curvature SSRF energy function.

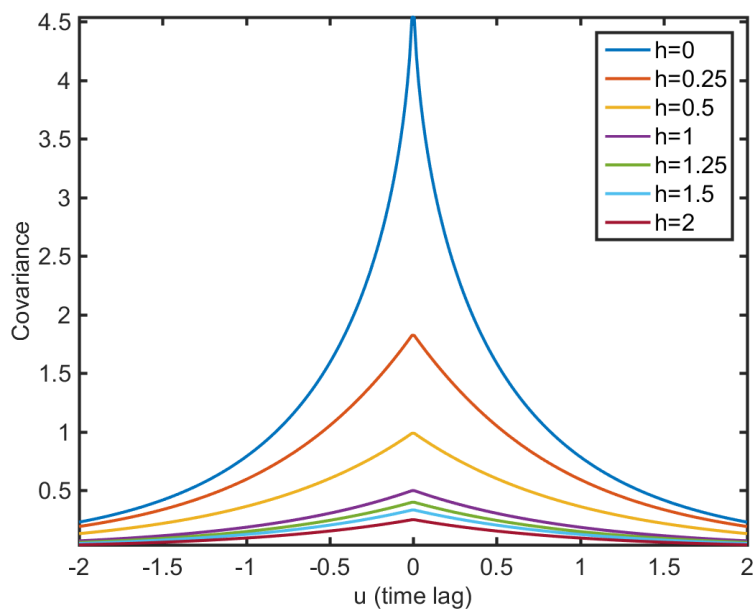


Figure 2: Parametric plots of the STSLR covariance (9) versus the normalized time lag u for different space lags h ; the space lag increases in the direction from top to bottom.

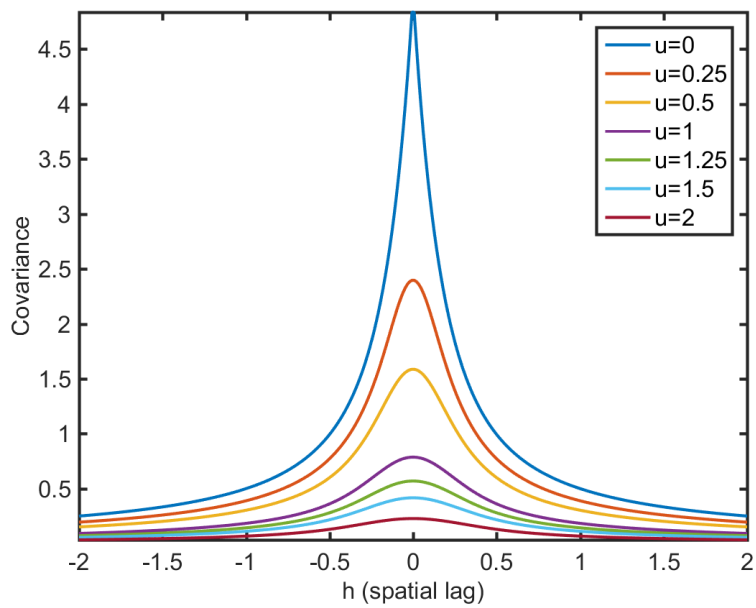


Figure 3: Parametric plots of the STSLR covariance (9) versus the normalized spatial lag h for different time lags u ; the time lag increases in the direction from top to bottom.

3.4.2 Continuity and differentiability

The STSLR covariance function (9) is continuous for every (normalized) space lag h (time lag u). We show this as follows: For all $u \in \mathbb{R}_{0,+}$ and $h \in \mathbb{R}_+$, the function $C_3(h, u)$ is continuous because it comprises products of everywhere continuous functions, e.g., $\exp(\cdot)$, $\operatorname{erf}(\cdot)$, and $\operatorname{erfc}(\cdot)$. The case $h = 0$ should be treated separately, because of the factor $1/h$ which diverges as $h \rightarrow 0$. The limit $h \rightarrow 0$ is evaluated in (14a) below, leading to the marginal covariance function $C_T(u)$ which is continuous for all $u \in \mathbb{R}_{0,+}$. Hence, the continuity of $C_3(h, u)$ is assured for all $h, u \in \mathbb{R}_{+,0}$.

In addition, each of the three summands in the covariance (9) involves either (i) $\operatorname{erf}(\cdot)$ or $\operatorname{erfc}(\cdot)$ and (ii) either $\exp(-u)/h$ or $\exp(\pm h)/h$. The functions (i) are everywhere differentiable, whereas the functions (ii) are non-differentiable at $h = 0$ or both $u = 0$ and $h = 0$ due to the presence of the absolute values in h and u .

The above continuity and differentiability properties imply that random fields with the covariance (9) are continuous but non-differentiable in the mean square sense [1].

Parametric plots of the STSLR covariance function $C_3(h, u)$ for fixed spatial lags are shown in Fig. 2 and for fixed time lags in Fig. 3. Note that $C_3(h, u)$ for fixed $u \neq 0$ appears smooth everywhere (including $h = 0$), while for every fixed h the function $C_3(h, u)$ has a cusp at the origin ($u = 0$).

This behavior is due to the fact that $C_3(h, u)$ admits a Taylor expansion around $h = 0$ for finite u but not around $u = 0$ for finite h . The Taylor expansion around $h = 0$ is given by

$$C_3(h, u) = \frac{\eta_0 \lambda}{2} \operatorname{erfc}(\sqrt{u}) + f_1(u) h^2 + f_2(u) h^4 + \mathcal{O}(h^6),$$

where the functions $f_i(u)$, $i = 1, 2, \dots$, diverge as $u \rightarrow 0$. However, for $u \neq 0$ the Taylor expansion is well defined and only involves terms $\mathcal{O}(h^{2n})$, where n is an integer. This property implies that the field fluctuations are smoother in space than in time [35].

A Taylor expansion is not possible around $u = 0$ even for $h \neq 0$, due to the presence of the factors $u^{-1/2}$ in the $\operatorname{erf}(\cdot)$ and $\operatorname{erfc}(\cdot)$ terms of the covariance function (9).

4 The STSLR Space-Time Variogram Function

In this section we derive the STSLR variogram that corresponds to the stationary covariance function (9) as well as expressions for the marginal time and space covariance and variogram functions.

The STSLR covariance function (9) is reduced to simpler expressions at zero spatial and temporal lag. These are useful in the estimation of the covariance parameters from space-time data. The spatial marginal STSLR function $C_S(h)$ and the temporal marginal STSLR function $C_T(u)$ are given by the following limits

$$C_T(u) \doteq \lim_{h \rightarrow 0} C_3(h, u). \quad (10a)$$

$$C_S(h) \doteq \lim_{u \rightarrow 0} C_3(h, u), \quad (10b)$$

Based on these, we also define the respective marginal spatial and temporal STSLR variogram functions as follows

$$\gamma_S(h) = C_S(0) - C_S(h), \quad \gamma_T(h) = C_T(0) - C_T(h). \quad (11)$$

4.1 Temporal marginal functions

To evaluate $C_T(u)$ based on the limit (10a) we use the Taylor series expansion of the error function around zero, i.e.,

$$\operatorname{erf}(x) = \frac{2}{\sqrt{\pi}} \left(x - \frac{x^3}{3} + \mathcal{O}(x^5) \right),$$

where the notation $\mathcal{O}(x^p)$ implies that the omitted terms are of order p or higher. Based on this expansion we evaluate the ratio of the error function over h as follows

$$\frac{1}{h} \operatorname{erf} \left(\frac{\lambda h}{2\sqrt{u}} \right) = \frac{\lambda}{\sqrt{\pi u}} + \mathcal{O}(h^2).$$

The above leads to an expression that is independent of h at the limit $h \rightarrow 0$, i.e.,

$$\lim_{h \rightarrow 0} \frac{e^{-u}}{2h} \operatorname{erf} \left(\frac{\lambda h}{2\sqrt{u}} \right) = \frac{\lambda e^{-u}}{2\sqrt{\pi u}}. \quad (12)$$

Similarly, we use the following Taylor expansion for the complementary error function around $h = 0$

$$\operatorname{erfc} \left(\sqrt{u} \pm \frac{\lambda h}{2\sqrt{u}} \right) = \operatorname{erfc}(\sqrt{u}) \mp \frac{\lambda h}{\sqrt{\pi u}} e^{-u} + \mathcal{O}(h^2).$$

In light of the above, the terms in the STSLR covariance (9) that involve the complementary error function behave at the limit $h \rightarrow 0$ as follows

$$\begin{aligned}
& \lim_{h \rightarrow 0} \frac{1}{4h} \left[e^{\lambda h} \operatorname{erfc} \left(\sqrt{u} + \frac{\lambda h}{2\sqrt{u}} \right) - e^{-\lambda h} \operatorname{erfc} \left(\sqrt{u} - \frac{\lambda h}{2\sqrt{u}} \right) \right] = \\
& \lim_{h \rightarrow 0} \left[\frac{\sinh(\lambda h)}{2h} \operatorname{erfc}(\sqrt{u}) - \frac{\lambda}{2\sqrt{\pi u}} e^{-u} \cosh(\lambda h) \right] \\
& = \frac{\lambda}{2} \operatorname{erfc}(\sqrt{u}) - \frac{\lambda}{2\sqrt{\pi u}} e^{-u}.
\end{aligned} \tag{13}$$

By combining the expansions for the covariance terms that are proportional to the error function and the complementary error function, i.e., equations (12) and (13), we obtain the following expressions for the temporal marginal covariance $C_T(u)$ and the temporal marginal variogram $\gamma_T(u)$

$$C_T(u) = \frac{\lambda \eta_0}{2} \operatorname{erfc}(\sqrt{u}), \tag{14a}$$

$$\gamma_T(u) = \frac{\lambda \eta_0}{2} [1 - \operatorname{erfc}(\sqrt{u})]. \tag{14b}$$

The dependence of $C_T(u)$ on the normalized time lag is illustrated in the parametric plot shown in Fig. 2 for $h = 0$. The marginal covariance $C_T(u)$ tends asymptotically to zero as $u \rightarrow 0$.

4.2 Spatial marginal functions

The marginal spatial covariance is obtained from (9). At zero temporal lag, i.e., $u \rightarrow 0$ and finite h the arguments of the error function and the complementary error function in (9) tend to infinity. Thus, taking into account that $\operatorname{erfc}(x) = 1 - \operatorname{erf}(x)$ as well as the limits $\lim_{x \rightarrow \infty} \operatorname{erf}(x) = 1$, $\lim_{x \rightarrow \infty} \operatorname{erfc}(x) = 0$ and $\lim_{x \rightarrow -\infty} \operatorname{erfc}(x) = 2$, we obtain the following expressions for the marginal spatial covariance and variogram functions

$$C_S(h) = \frac{\eta_0}{2h} (1 - e^{-\lambda h}), \tag{15a}$$

$$\gamma_S(h) = \frac{\eta_0}{2} \left[\lambda - \frac{1 - \exp(-\lambda h)}{h} \right]. \tag{15b}$$

The dependence of $C_S(h)$ on the normalized spatial lag is illustrated in the parametric plot shown in Fig. 3 for $u = 0$.

4.3 The STSLR Variogram Function

The space and time marginal covariances tend both to the variance as the respective lag tends to zero, i.e., $\lim_{h \rightarrow 0} C_S(h) = \lim_{u \rightarrow 0} C_T(u) = \sigma_x^2$. Hence, as it follows from (15a) and (14a) the variance of the spatiotemporal random field is $\sigma_x^2 = \eta_0 \lambda / 2$. Consequently, the STSLR variogram function is given by

$$\gamma(h, u; \tilde{\theta}) = \frac{\eta_0 \lambda}{2} - C_3(h, u; \tilde{\theta}), \quad (16)$$

where $C_3(h, u; \tilde{\theta})$ is given by (9) and $\tilde{\theta}^\top = (\eta_0, \lambda, \xi, \tau_c)$.

5 Estimation

In this section we discuss the estimation of the parameters $\tilde{\theta}$ of the STSLR variogram from available space-time data. In principle it is possible to use maximum likelihood to estimate the optimal parameters from the data. However, maximum likelihood is computationally intensive due to memory storage requirements which scale as $\mathcal{O}(N^2)$, and the computational complexity of the covariance inversion which scales as $\mathcal{O}(N^3)$ for dense matrices, where N is the sample size. There exist methods that address the computational burden of maximum likelihood estimation by means of approximations or by dividing the problem in smaller pieces [36, 13]. Herein, we opt for a modified method of moments which is based on the marginal variograms and is simple to implement [4].

We assume that there are N_T time instants and that N_S is the total number of spatial locations (stations) that report a measurement at least at one time instant. The data involves the measurements $x_{i(j),j}$ where $j = 1, \dots, N_T$ is the time index, and $i(j) \in \{1, \dots, N_S\}$ is the space index. We assume a fixed time step δt , so that $t_j = j \delta t$, for $j = 1, \dots, N_T$. The normalized time lag then is $u_k = k \delta t / \tau_c$, where $k = 0, \dots, N_T - 1$.

For each time instant t_j , $j = 1, \dots, N_T$, we assume that there exists at least one measurement, e.g., at the location $\mathbf{s}_{i(j)}$ where $i(j) \in \{1, \dots, N_S\}$. We denote by S_j the set of points in space for which there are measurements at time t_j . This set comprises the locations $S_j = \{\mathbf{s}_{i(j)}\}$ where $i(j) \in \{1, \dots, N_S\}$. The cardinal number of the set is $N_j = \#S_j$. Since not all the stations have data at all times, it holds that $N_j \leq N_S$. Let us also denote by $S_{j,m} = S_j \cap S_m$ the set of spatial locations with measurements at both times t_j and t_m , and by $N_{j,m} = \#(S_j \cap S_m)$ the cardinal number of this set.

We estimate the empirical *temporal marginal variogram* as follows

$$\hat{\gamma}_t(t_m, t_{m+k}) = \frac{1}{2N_{m+k,m}} \sum_{\mathbf{s}_{i(m)} \in S_m} \mathbb{I}_{S_{j,m}} \delta_{j,m+k} [x_{i(m),j} - x_{i(m),m}]^2, \quad (17a)$$

$$\text{for } m = 1, \dots, N_T - k, \quad k = 1, \dots, \lfloor p N_T \rfloor,$$

$$\hat{\gamma}_T(u_k) = \frac{1}{N_S - k} \sum_{m=1}^{N_S - k} \hat{\gamma}_t(t_m, t_{m+k}). \quad (17b)$$

The indicator function $\mathbb{I}_{S_{j,m}}$ takes values $\mathbb{I}_{S_{j,m}} = 1$ if both \mathbf{s}_m and \mathbf{s}_j belong to the set $S_{j,m}$ and $\mathbb{I}_{S_{j,m}} = 0$ otherwise. The Kronecker delta, $\delta_{i,j} = 1$ if $i = j$ and $\delta_{i,j} = 0$ if $i \neq j$, restricts the respective average to times t_j and t_m such that $j = m + k$. Hence, the function $\hat{\gamma}_t(t_m, t_{m+k})$ is a purely spatial average over different locations for two specific times which are k steps apart. The maximum lag is defined as a fraction $0 \leq p \leq 1$ of N_T , where $\lfloor p N_T \rfloor$ denotes the largest integer that does not exceed $p N_T$. The function $\hat{\gamma}_T(t_m, t_{m+k})$ is a temporal average of $\hat{\gamma}_t(t_m, t_{m+k})$ over all pairs of time instants that are k steps apart.

Similarly, we define the estimator of the *spatial marginal variogram* as follows

$$\hat{\gamma}_s(\mathbf{s}_\alpha, \mathbf{s}_\beta) = \frac{1}{2N_{\alpha,\beta}} \sum_{j=1}^{N_S} \mathbb{I}_{j;\alpha,\beta} (x_{\alpha,j} - x_{\beta,j})^2, \quad \alpha, \beta = 1, \dots, N_S \quad (18a)$$

$$N_{\alpha,\beta} = \sum_{j=1}^{N_T} \mathbb{I}_{j;\alpha,\beta}, \quad (18b)$$

$$\hat{\gamma}_S(\mathbf{r}) = \frac{1}{N_s(\mathbf{r})} \sum_{\alpha=1}^{N_S} \sum_{\beta=1}^{N_S} \hat{\gamma}_s(\mathbf{s}_\alpha, \mathbf{s}_\beta) \mathbb{I}_{\mathbf{s}_\alpha, \mathbf{s}_\beta \in B_\epsilon(\|\mathbf{r}\|)}. \quad (18c)$$

In the above, $\mathbb{I}_{j;\alpha,\beta}$ is an indicator function such that $\mathbb{I}_{j;\alpha,\beta} = 1$ if both locations \mathbf{s}_α and \mathbf{s}_β have measurements at the time instant t_j and $\mathbb{I}_{j;\alpha,\beta} = 0$ otherwise. $\mathbb{I}_{\mathbf{s}_\alpha, \mathbf{s}_\beta \in B_\epsilon(\|\mathbf{r}\|)}$ is an indicator function that equals one if the endpoint of the lag vector $\mathbf{s}_\alpha - \mathbf{s}_\beta$ is inside the neighborhood of the vector \mathbf{r} , which is defined in terms of a specified tolerance ϵ .

By fitting $\hat{\gamma}_T(u_k)$ to the STSLR marginal temporal variogram (14b) we estimate the characteristic time τ_c and the product $\lambda \eta_0$. Then, by fitting $\hat{\gamma}_S(\mathbf{r})$ to the marginal spatial STSLR variogram (15b) we estimate λ and the spatial characteristic length ξ . Finally, using the estimate of the product $\lambda \eta_0$ from the fit of the marginal temporal STSLR variogram, we estimate η_0 .

c_0	c_1	c_2	$c_{1,1}$	$c_{2,2}$	$c_{1,2}$	R	p
-4.44	$-9.25 \cdot 10^{-4}$	-0.035	$-1.56 \cdot 10^{-5}$	$-4.3 \cdot 10^{-5}$	$-2.49 \cdot 10^{-6}$	0.455	$1.6 \cdot 10^{-29}$

Table 1: Coefficients of the quadratic trend regression model (19), as well as the value of the correlation coefficient R between the trend and the data, and the p value of the trend model.

6 Application to Ozone Data

We use a set of daily concentration values of atmospheric ozone over the conterminous USA (excluding Alaska and Puerto Rico), which were downloaded from the US Environmental Protection Agency Air Data website [2]. The data involve daily averages of ozone levels at 629 stations sampled over 14 consecutive days starting on January 1, 2015 (daily summary data file 44201 2015). The daily averages are based on eight measurements per day. The ozone concentration is measured in parts per million (ppm) in volume. For the purpose of the analysis below the ozone concentrations have been multiplied by 100.

The spatial distribution of the locations and the ozone levels are shown in Fig. 4. Maps of approximate ozone concentrations are obtained by means of natural neighbor interpolation [12] and they are displayed in Fig. 5. Based on the visual inspection of these maps we postulate a quadratic spatial trend function. The latter is modeled by the second degree polynomial

$$m(\mathbf{s}) = c_0 + c_1 s_1 + c_2 s_2 + c_{1,1} s_1^2 + c_{2,2} s_2^2 + c_{1,2} s_1 s_2, \quad (19)$$

where $\mathbf{s} = (s_1, s_2)$ are the location vectors on the plane. The spatial coordinates of the station locations have been converted to the World Geodetic System 1984 (WGS84) from the initial longitude-latitude format. Subsequently, the spatial coordinates have been normalized by dividing with 10^4 m.

The coefficients of the optimal (in the least squares sense) trend model are given in Table 1. Most of the coefficients have negative values even though the ozone concentrations are positive. The sign of the coefficients is due to the preponderance of negative values among the spatial coordinates of the stations.

We use the detrended ozone data to estimate the marginal variograms according to (17) and (18). The empirical temporal marginal variogram and its fit to the theoretical STSLR marginal function (14b) is shown in Fig. 6. The empirical omnidirectional spatial marginal variogram and the respective fit to the theoretical STSLR marginal function (15b) is shown in Fig. 7. The estimated parameters for the STSLR variogram model are as follows: $\eta_0 = 0.7924 \text{ ppm}^2 \times 10^4$, $\lambda = 1.07$ (dimensionless flexibility), $\xi = 45.49$ in normalized units (equivalently $\xi \approx 450\text{km}$), $\tau_c = 4.70$ days.

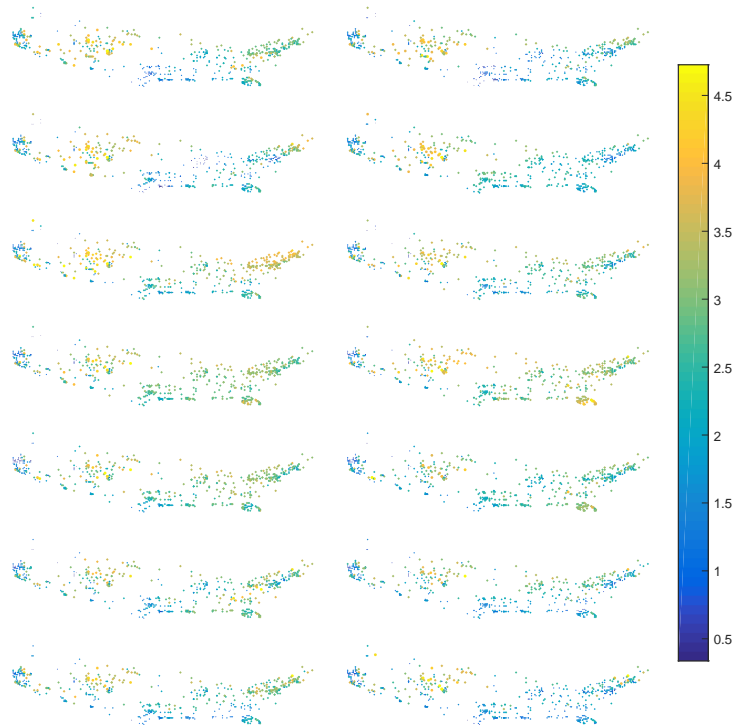


Figure 4: Ozone daily average levels measured over the conterminous USA for 14 consecutive days in 2015 starting on January 1, 2015. The colorbar scale corresponds to ozone concentration levels multiplied by 100. The actual ozone levels (in ppm) are obtained by multiplying the colorbar scale with 10^{-2} . According to EPA the air quality standard for ozone is 0.075 ppm, averaged over eight hours.

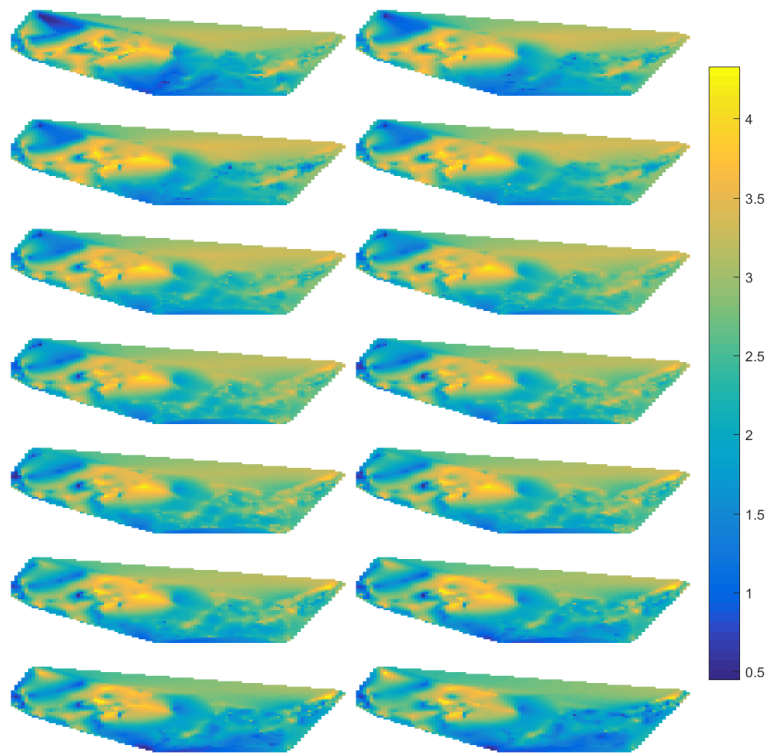


Figure 5: Maps of ozone concentration on a 100×50 map grid based on natural neighbor interpolation of the data shown in Fig. 4.

The empirical spatial marginal variogram includes a nugget term with an estimated variance $c_0 = 0.4125$, while the nugget is negligible in the case of the temporal marginal variogram. The characteristic length ξ may seem high. However, it agrees with the smooth maps produced by means of natural neighbor interpolation in Fig. 5. The average distance between each station and its closest neighbor is 3.28 (32.8km) while the maximum distance between nearest neighbors is 26.74 (267.4km) in normalized units (km). This relatively large separation between stations accounts for the loss of spatial resolution during ozone sampling. This effect is also apparent in the finite nugget of the marginal spatial variogram.

The non-separable space-time STSLR variogram (16) based on the estimated optimal parameters for the ozone data is shown in Fig. 8 including the spatial nugget component. The projection on the plane $\|\mathbf{x}\| = 0$ represents the marginal STSLR time variogram without a nugget. The marginal STSLR time variogram is estimated by averaging the temporal variograms of the ozone time series at each location, and thus it does not incorporate spatial variability; the latter appears as a discontinuity for $\|\mathbf{x}\| > 0$. The nugget term explains the difference between the sills of the marginal time and space variograms in the plot, since the sills of the STSLR marginal variograms are identical by construction.

7 Discussion and Conclusions

There is an ongoing interest in the development of flexible and realistic spatiotemporal covariance functions. We explore the generation of non-separable space-time covariance functions based on the solutions of respective equations of motion. The latter are partial differential equations that follow from the theory of linear response which describes the dynamic fluctuations of random fields around an equilibrium point.

The covariance equation of motion (4) is based on an equilibrium “energy function” determined by the squares of the fluctuating field, its gradient, and its curvature. Combining the explicit solution in one spatial dimension of the covariance equation of motion (4) with the turning bands method, we obtain the novel STSLR space-time covariance (9) which comprises a combination of exponential factors, error functions, and algebraic powers. The STSLR covariance is a non-separable, space-time stationary, and spatially isotropic function which does not belong in the Gneiting class. In addition, the STSLR space-time covariance is everywhere continuous but non-differentiable at zero space and/or time lag.

The STSLR space-time covariance includes four parameters: an overall scale factor, η_0 , a characteristic time, τ_c , a characteristic length, ξ , and a flexibility coefficient, λ , which is related to the “resistance” of the spatial fluctuations to spatial

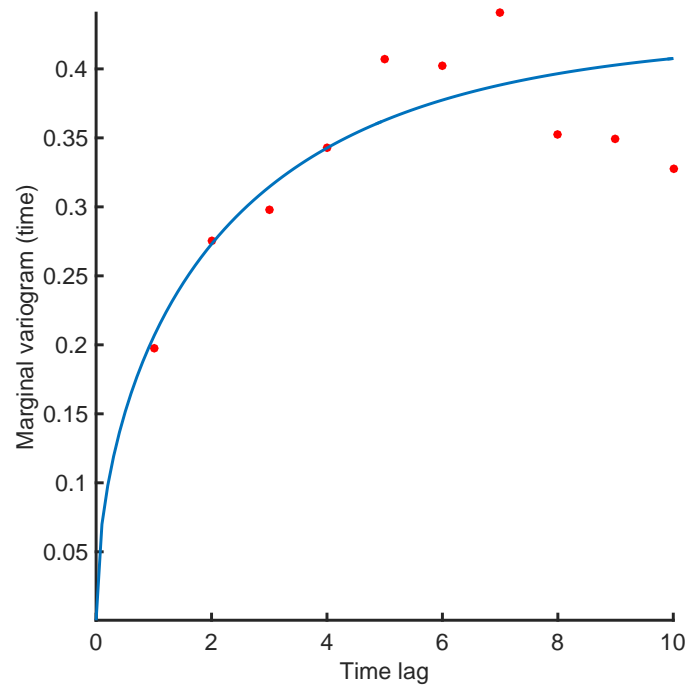


Figure 6: Marginal temporal variogram estimated from the data (circles) and best fit to the theoretical STSLR temporal model (14b). The time lag is measured in terms of days. The vertical axis is measured in $\text{ppm}^2 \times 10^4$.

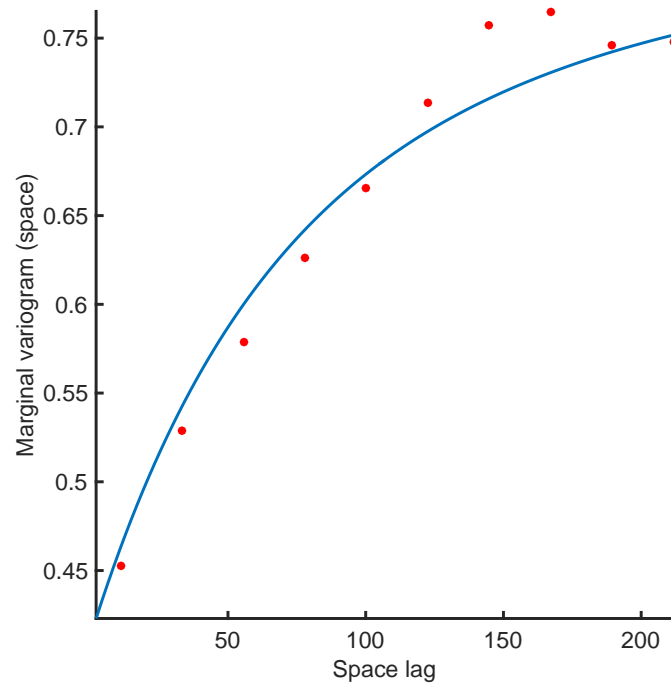


Figure 7: Marginal spatial variogram estimated from the data (circles) and best fit to the theoretical STSLR spatial model (15b). The actual spatial lag is obtained by multiplying the horizontal axis with 10^4m . The units of the vertical axis are $\text{ppm}^2 \times 10^4$.

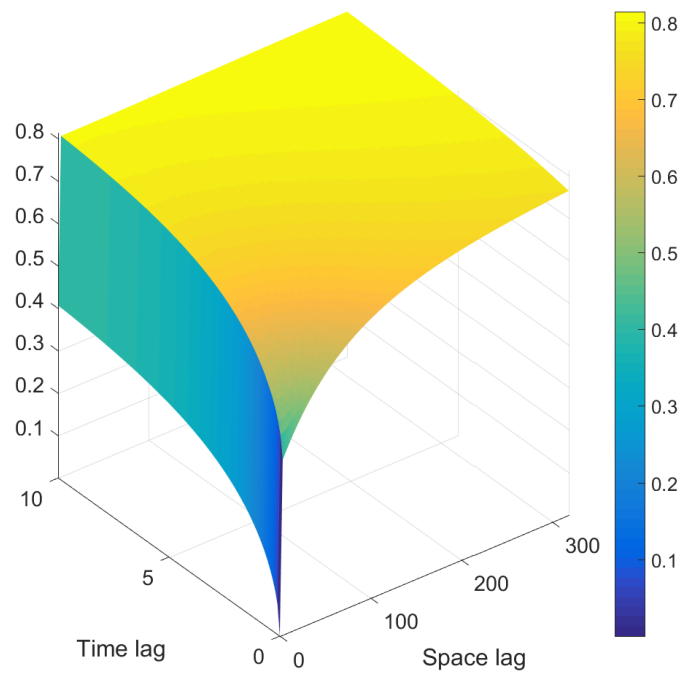


Figure 8: Space-time variogram model for the ozone data which consists of the STSLR space-time model (16) and a spatial nugget term. The time lag is measured in days, and the spatial lag has been normalized by dividing with 10^4m . The vertical axis is measured in $\text{ppm}^2 \times 10^4$.

gradients. Larger values of λ imply that the random field is more likely to admit higher gradients than for lower λ . In addition, it is possible to incorporate geometric anisotropy by means of rotation and scaling transformations of the spatial lag vector in (9), e.g. [5]. Future research will focus on developing efficient interpolation and simulation schemes based on the STSLR covariance function as well as comparisons with other covariance models.

A more general question is whether the linear response theory can be extended to include solutions of hyperbolic type. Another interesting problem is whether a tractable solution of (4) can be derived in three spatial dimensions, in order to avoid the application of the turning bands transform. A solution has been obtained at the zero-curvature limit, but this function diverges at $\|\mathbf{r}\| = 0$ [21]. A finite curvature term is needed in order to overcome the divergence. However, the integral of the spectral density for finite curvature is not analytically tractable, which means that a closed-form expression can at best be derived as a series expansion. Such an expansion may lead to more flexible parametric covariance forms.

Acknowledgments

The research presented in this manuscript was partly funded by the project SPARTA 1591: “Development of Space-Time Random Fields based on Local Interaction Models and Applications in the Processing of Spatiotemporal Datasets”. The project SPARTA was implemented under the “ARISTEIA” Action and was co-funded by the European Social Fund and National Resources.

References

- [1] R. Adler. *The Geometry of Random Fields*. Society for Industrial and Applied Mathematics, 2010.
- [2] US Environmental Protection Agency. Air Quality System Data Mart [internet database]. <https://www.epa.gov/airdata>. Accessed: 2016-07-08.
- [3] S. Bochner. *Lectures on Fourier Integrals*. Princeton University Press, Princeton, NJ, 1959.
- [4] L. De Cesare, D. E. Myers, and D. Posa. Estimating and modeling space–time correlation structures. *Statistics & Probability Letters*, 51(1):9–14, 2001.

- [5] A. Chorti and D. T. Hristopulos. Nonparametric identification of anisotropic (elliptic) correlations in spatially distributed data sets. *IEEE Transactions on Signal Processing*, 56(10):4738–4751, 2008.
- [6] G. Christakos. *Random Field Models in Earth Sciences*. Academic Press, San Diego, 1992.
- [7] G. Christakos and D. T. Hristopulos. *Spatiotemporal Environmental Health Modelling*. Kluwer, Boston, 1998.
- [8] N. Cressie and C. L. Wikle. *Statistics for Spatio-temporal Data*. John Wiley and Sons, New York, 2011.
- [9] S. De Iaco, D. Myers, and D. Posa. Nonseparable space-time covariance models: some parameteric families. *Mathematical Geology*, 34(1):23–42, 2002.
- [10] M. R. Dennis, P. Glendinning, P. A. Martin, F. Santosa, J. Tanner, and N. J. Higham. *The Princeton Companion to Applied Mathematics*. Princeton University Press, Princeton, NJ, 2015.
- [11] L. Ehrenpreis. *The Universality of the Radon Transform*. Oxford University Press on Demand, 2003.
- [12] P. Fisher, H. Ledoux, and C. Gold. An efficient natural neighbour interpolation algorithm for geoscientific modelling. In *Developments in Spatial Data Handling*, pages 97–108. Springer Berlin Heidelberg, 2005.
- [13] M. Fuentes. Approximate likelihood for large irregularly spaced spatial data. *Journal of the American Statistical Association*, 102(477):321–331, 2007.
- [14] R. Ghanem and P. D. Spanos. *Stochastic Finite Elements: A Spectral Approach*. Dover, 2003.
- [15] T. Gneiting. Nonseparable, stationary covariance functions for space–time data. *Journal of the American Statistical Association*, 97(458):590–600, 2002.
- [16] V. Heine. Models for two-dimensional stationary stochastic processes. *Biometrika*, 42(1-2):170–178, 1955.
- [17] P. C. Hohenberg and B. I. Halperin. Theory of dynamic critical phenomena. *Reviews of Modern Physics*, 49:435–479, 1977.

- [18] D. T. Hristopulos. Spartan Gibbs random field models for geostatistical applications. *SIAM Journal on Scientific Computing*, 24(6):2125–2162, 2003.
- [19] D. T. Hristopulos. Covariance functions motivated by spatial random field models with local interactions. *Stochastic Environmental Research and Risk Assessment*, 29:739–754, 2015.
- [20] D. T. Hristopulos and S. Elogne. Analytic properties and covariance functions of a new class of generalized Gibbs random fields. *IEEE Transactions on Information Theory*, 53(12):4667–4679, 2007.
- [21] D. T. Hristopulos and I. C. Tsantili. Space-Time models based on random fields with local interactions. *International Journal of Modern Physics B*, 29:1541007, 2015.
- [22] D. T. Hristopulos and M. Žukovič. Relationships between correlation lengths and integral scales for covariance models with more than two parameters. *Stochastic Environmental Research and Risk Assessment*, 25(2):11–19, 2011.
- [23] D.T. Hristopulos. Spartan Gibbs random field models for geostatistical applications. *SIAM Journal of Scientific Computing*, 24(6):2125–2162, 2003.
- [24] R. H. Jones and Y. Zhang. Models for continuous stationary space-time processes. In *Modelling longitudinal and spatially correlated data*, pages 289–298. Springer, 1997.
- [25] A. C. King, J. Billingham, and S. R. Otto. *Differential Equations: Linear, Nonlinear, Ordinary, Partial*. Cambridge University Press, Cambridge, 2003.
- [26] A. Kolovos, G. Christakos, D.T. Hristopulos, and M. L. Serre. Methods for generating non-separable spatiotemporal covariance models with potential environmental applications. *Advances in Water Resources*, 27(8):815–830, 2004.
- [27] B. Li, M. G. Genton, and M. Sherman. A nonparametric assessment of properties of space–time covariance functions. *Journal of the American Statistical Association*, 102(478):736–744, 2007.
- [28] F. Lindgren and H. Rue. Bayesian spatial modelling with R-INLA. *Journal of Statistical Software*, 63(19), 2015.
- [29] F. Lindgren, H. Rue, and J. Lindström. An explicit link between Gaussian fields and Gaussian Markov random fields: The SPDE approach. *Journal of the Royal Statistical Society, Series B*, 73(4):423–498, 2011.

- [30] C. Ma. Families of spatio-temporal stationary covariance models. *Journal of Statistical Planning and Inference*, 116(2):489–501, 2003.
- [31] C. Ma. Recent developments on the construction of spatio-temporal covariance models. *Stochastic Environmental Research and Risk Assessment*, 22(1):S39–S47, 2008.
- [32] A. Mantoglou and J. L. Wilson. The turning bands method for simulation of random fields using line generation by a spectral method. *Water Resources Research*, 18(5):1379–1394, 1982.
- [33] G. Matheron. The intrinsic random functions and their applications. *Journal of Applied Probability*, 5(3):439–468, 1973.
- [34] E. W. Ng and M. Geller. A table of integrals of the error functions. *Journal of Research of the National Bureau of Standards B*, 73(1):1–20, 1969.
- [35] M. L. Stein. Space–time covariance functions. *Journal of the American Statistical Association*, 100(469):310–321, 2005.
- [36] M. L. Stein, Z. Chi, and L. J. Welty. Approximating likelihoods for large spatial data sets. *Journal of the Royal Statistical Society: Series B (Statistical Methodology)*, 66(2):275–296, 2004.
- [37] P. Whittle. On stationary processes in the plane. *Biometrika*, 41(3/4):434–449, 1954.
- [38] D. Xiu and G. Em. Karniadakis. Modeling uncertainty in flow simulations via generalized polynomial chaos. *Journal of Computational Physics*, 187(1):137–167, 2003.
- [39] A. M. Yaglom. Some classes of random fields in n -dimensional space, related to stationary random processes. *Theory of Probability and its Applications*, 2(3):273–320, 1957.
- [40] A. M. Yaglom. *Correlation Theory of Stationary and Related Random Functions I*. Springer Verlag, New York, 1987.